Cavitation clusters in lipid systems – ring-up, bubble population, and bifurcated streamer lifetime

P. R. Birkin,[a†] J. J. Youngs[a], T. T. Truscott[b], and S. Martini[c]

Abstract

The processing of oils is vital to their ultimate use within the food industry. Control over the physical properties of such materials could be achieved through the application of high-intensity ultrasound (HIU). However the exact mechanism, centred upon acoustic cavitation, is currently unclear. The ring-up of a HIU source in an oil media is studied in the presence and absence of a pre-exsisting bubble population. High-speed imaging and acoustic measurements within the system is demonstrated to be extremely useful in characterising the dynamics present under non steady-state conditions. The behaviour of the clusters generated in the first 1000 ms under these conditions is shown to be signifigantly different depending on the bubble population. A bifurcated streamer (BiS), originating from a unique bi-cluster event, is only observable in the presence of a bubble population during the ring-up process to higher cluster orders. In addition, the lifetime of this BiS event is highly temperature dependent and is shown to be a good marker for the viscosity of the oil employed.

Keywords: bubble population, ring-up, clusters, oil, processing, lifetime

[†]Corresponding author, prb2@soton.ac.uk

[a]Chemistry, University of Southampton, Southampton, UK, S0171BJ.

[b]Department of Mechanical and Aerospace Engineering, Utah State University, Logan, UT, 84322-4130, USA.

[c]Department of Nutrition, Dietetics, and Food Science, Utah State University, Logan, UT, 84322-8700, USA.

Introduction

The processing of food materials possess significant technological challenges. Many different strategies exist with new processes developed to improve the properties of the resultant material. For example, edible lipids which provide flavour, mouthfeel, and palatability to foods, can be affected by the processing conditions. In many cases, the desired properties can be achieved through control of the amount of solidified lipids and the characteristics of the crystalline network formed. One promising technology which has been shown to change the properties of the resultant solid materials formed, when it is used as part of the solidification process, is high intensity ultrasound (HIU)[1–6]. The positive effects of this technology are thought to be associated with its ability to alter the kinetics of crystallisation within these oil matrixes[7–14]. Unfortunately, the exact physical or chemical processes responsible for the changes observed are unknown at this time. However, considering the possible mechanisms available, the role of cavitation[15–18] in these systems cannot be overlooked. Hence, an understanding of the cavitation processes generated through the application of HIU to an edible oil is timely. To this end, characterisation of the clusters[19,20] and streamer formed at the tip of a HIU source has been reported[21,22]. These studies have shown a rich and complex environment which is dynamic and exhibits different characteristics depending on the amplitude of the HIU source and the state of the tip itself. In addition, local heating and the dynamics of clusters of bubbles at the tip of the HIU source are important[22,23]. While these studies are significant, they have focused on the behaviour of the cavitation field under steady state conditions (where the tip has been operational for a few seconds). While this gives many details on the physical processes associated with the HIU source, there remains several key questions. First, as the effects of HIU are dramatic and occur with short exposure time (~10 s), it is unclear what happens in the initial stages of the exposure to ultrasound. Second, how does the pre-treatment and bubble population of the oil affect these processes? Lastly, how do the physical characteristics of the oil itself affect the cavitation process? To gather this key information, it is necessary to study the environment and bubble dynamics with suitable analytical methods. Here we use acoustic emission and high-speed imaging to gain insight into the processes occurring under non-steady state conditions (e.g. at initiation of the HIU source). The results reported will show that the dynamics of the cavitation clusters and the lifetimes of the types of bubble events generated depend strongly on the physical conditions[24–28] employed, the pre-existing bubble population and the timescale of the excitation.

Experimental

The experimental set up has been described in some detail previously[23]. Cavitation was generated using a piston like emitter (PLE, Misonix, XL2000, ~23 kHz) immersed in the relevant media here an oil (Soybean oil, SBO (Clearsprings) or Sunflower oil, SFO (Independent)). A 3.2 mm diameter tip was employed in all cases. The tip of the PLE was not polished as this was found not to be conducive to the formation of stable clusters in these oil systems (see reference[21]). High-speed imaging (using a Photron APX-RS camera and Navitar x12 lens, typically at 70 kfps and a shutter speed of 14.3 μs) of the region below the tip in the oil system was combined with a calibrated hydrophone (Reson TC4013) positioned ~ 15 mm to the side of the tip of the probe (itself 15 mm immersed into the oil). The sensitivity of this sensor is given as -2.66 x 10^{-5} V Pa^{-1} under these conditions at ~22.7 kHz in water (from the data sheet provided from the manufacturer[29]), however, the calibration of the hydrophone is assumed not to be 100% accurate within the oil system. Characterisation of the PLE was achieved with two alternate. First, through standard calorimetry (see ref[21] SI data). Second, through monitoring the tip amplitude (see ref [22]and SI). In addition, a set of ring-up data and accompanying audio traces are available in the SI.

A 60 mm x 60 mm x 150 mm polycarbonate cell was used to contain the liquid for imaging experiments. A 70 mm x 70 mm x 170 mm water jacketed cell (See SI) was used with a water bath (Grant, TC120) to allow temperature control for the BiS lifetime experiments. Viscosity data was collected by using AR-G2 Rheometer (TA Instruments, New Castle, Delaware) to identify steady state flow at varying shear rates (0.01-300 s^{-1}). A digital oscilloscope (Owon DS7102V DSO) was used to capture the acoustic and light scattering data (sample rate 1 MHz). The scope, ultrasonic source (through a relay) and the high-speed camera were triggered by a TTL pulse generated by a suitable voltage source.

A similar approach used to measure light scattering through the cluster has been described elsewhere for water based experiments[30,31]. DSP analysis was performed using a bespoke data analysis program (Microsoft Visual Basic 2010 and National Instruments Measurement Studio). In this an FFT analysis was performed with a window size chosen to allow many cycles (usually 100 or 1000) of the PLE period to be analysed at one time. This window was then sequentially moved forward through the data in 1 ms steps. The output of this process was then used to produce a plot of the intensity of a particular frequency component as a function of time. This approach is particularly useful as it enables the frequency components (particularly those related to shock emission as the result of cluster collapse) to be monitored and displayed.

Results and discussion

One of the experimentally observable characteristics of these lipid systems is that a set of clear audible 'notes' which can be detected by ear as the drive characteristics of the sound source are altered[22,23]. In brief as the drive amplitude was increased the cluster dynamics were

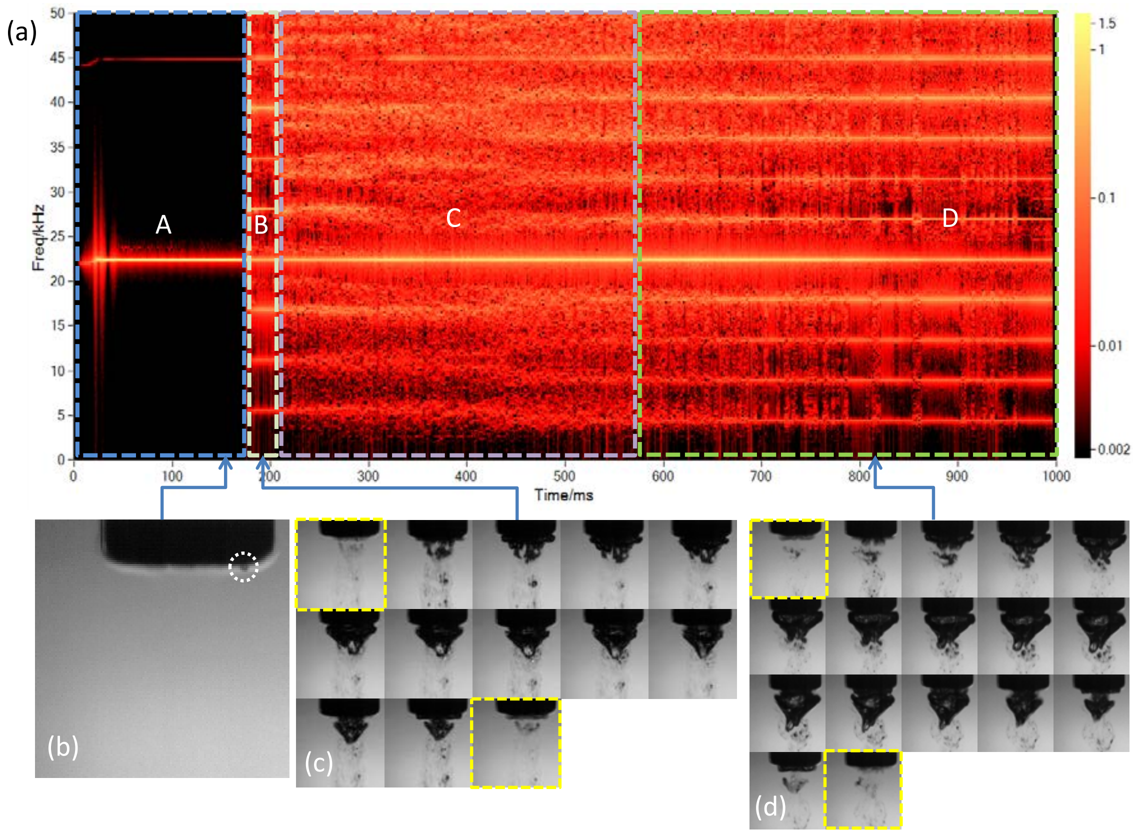

Figure 1. Panel (a) shows the frequency components (note the colour scale is in volts) of the signal recorded by the hydrophone as a function of time as the PLE was initiated (32 W_{rms}) in sunflower oil. The TTL trigger for the PLE and high-speed camera was initiated at Time = 0 s. The panel is split into different time regions where the FFT analysis shows distinct and different behaviour (labelled A-D and correlated to the discussion in the text). Panel (b) shows a single image of the PLE where the first bubble activity was observed. This occurred at 178.414 ms after the TTL trigger. The PLE is 3.2 mm in diameter and can be used as a scale for the images. Panel (c) shows the cluster dynamics and periodicity recorded in section B from panel (a). The high-speed imaging (70 kfps) shows a cluster periodicity corresponding to *f*/4 (shown as the yellow highlighted frames). Panel (d) shows the cluster dynamics and periodicity recorded in section D from panel (a). The high-speed imaging (70 kfps, shutter speed 14.3 μs) shows a cluster periodicity corresponding to *f*/5 (shown as the yellow highlighted frames). The blue arrows link the lower panels (b-d) to panel (a).

found to exhibit periodicities of differing order with respect to the frequency of the PLE deployed. The order can be defined as *f*/n where f is the drive frequency of the PLE and n is an integer value, typically 2-7. However, these experiments relied on the PLE operating under steady state (or continuous) conditions. Alternatively, how these clusters develop over time and how the pre-treatment of the oil (the bubble population for example) affects the behaviour seen is of interest. This has the potential to provide an enhanced understanding of the mechanisms present during HIU treatment lipid crystallisation, particularly at short timescales. To investigate this a set of complimentary experiments were undertaken. High-speed imaging and acoustic data were recorded simultaneously to correlate the observed pressure signals to the dynamics of the cluster (or cavitation events) at the surface of the PLE.

Figure 1 shows the results obtained from such an experiment. In this case, the oil had been allowed to rest for ~ 1-2 hours without disturbance (e.g. exposure to cavitation conditions or flow). Initially after a ~5 ms delay (because of the activation of the ultrasonic power amplifier through a relay), an acoustic signal, predominately at 22.68 kHz, was detected. This signal grew in amplitude until ~ 180 ms into the experiment (this time zone is marked on panel (a) as section A). High-speed imaging during this time revealed a bubble-free liquid until ~178 ms into the experiment. At this point a single bubble nucleated at the surface of the PLE (see Figure 1 (b)). After this event had occurred, multiple bubble events were detected, and the acoustic signature and its corresponding frequency space character altered dramatically (see Figure 1 sections B, C and D). Figure 1 panel (a) section B then indicates a set of subharmonics (and corresponding ultraharmonics) with an *f*/4 cluster. In this region the high-speed imaging shows a well-developed cluster with a repeating period corresponding to *f*/4 (see Figure 1 panel (c), where the highlighted frames, read left to right in a raster fashion from the top). This cluster behaviour results in 3 subharmonic peaks at *f*/4, *f*/2, and 3*f*/4. However, this cluster last for only ~ 30 ms after which time the frequency analysis shows an ill-defined emission lasting for ~ 350 ms (see Figure 1, Panel (a) section C) where no clear sub or ultraharmonics were detected. At ~575 ms Figure 1 panel (a) and (d) shows the formation of an *f*/5 cluster. This is highlighted in Figure 1 panel (d) by the yellow boxes which show the period of the cluster which is estimated to be ~16 ± 1 frames or 220 μs. It should be noted that this behaviour is only detected when the liquid has been allowed to stand for an extended time period (~ 1-2 hours) to enable as many bubbles as possible to be removed through buoyancy forces or dissolution effects.

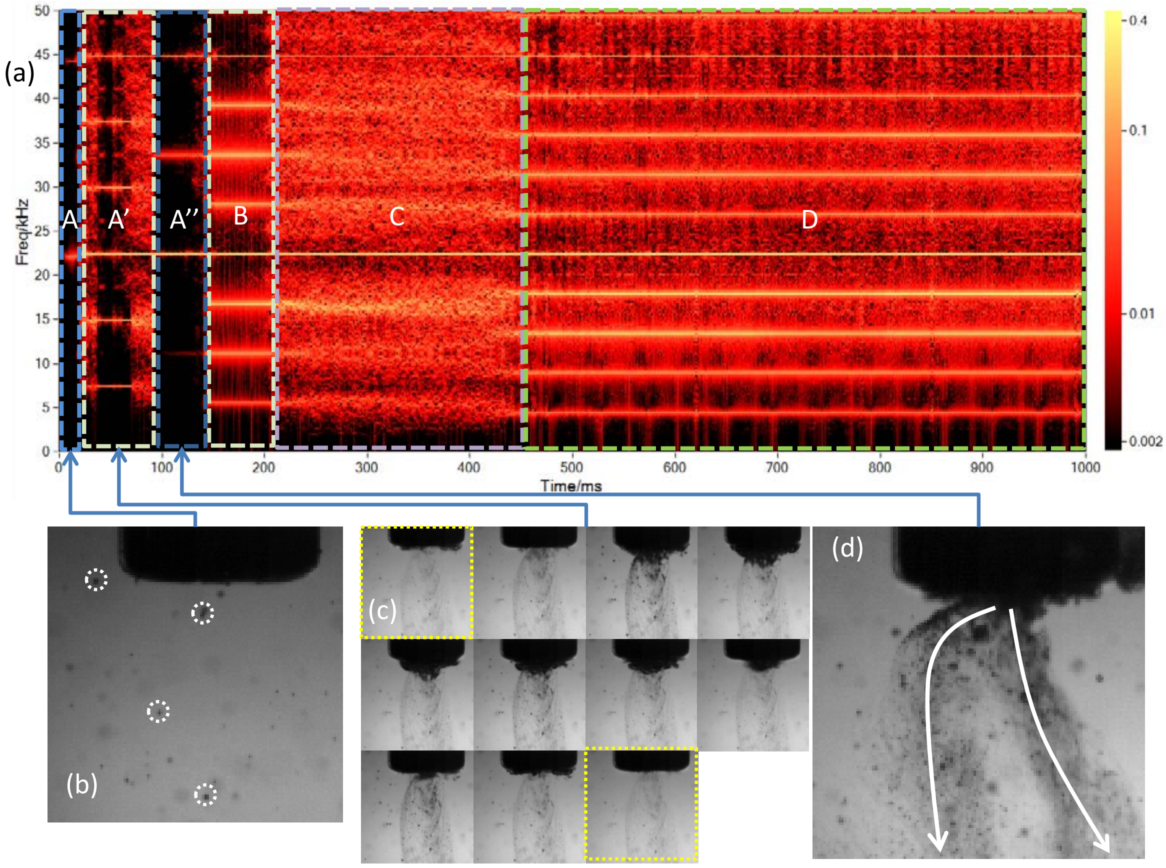

Figure 2. Panel (a) shows the frequency components of the signal recorded by the hydrophone as a function of time as the PLE was initiated (32 W_{rms}) in sunflower oil pre-populated with gas bubbles through exposure to cavitation generated by the PLE. The TTL trigger for the PLE and high-speed camera was initiated at t = 0 s. The panel is split into different time regions where the FFT analysis shows distinct behaviour (labelled A, A', A'', B-D and correlated to the discussion in the text). Panel (b) shows a single image of the system prior to initialisation of the PLE. The white dotted circles show the presence of many gas bubbles which appear stationary on the time scale of the experiment. The PLE is 3.2 mm in diameter and can be used as a scale. Panel (c) shows the cluster dynamics and periodicity recorded in section A' from panel (a). The high-speed imaging (70 kfps, shutter speed = 14.3 μs) shows a cluster periodicity corresponding to *f*/3 (shown as the yellow highlighted frames). Panel (d) shows the cluster and streamer dynamics and periodicity recorded in section A'' from panel (a). The white arrows show the bifurcated streamer observed under these conditions. The blue arrows link the lower panels (b-d) to panel (a).

Figure 2 shows the results of a ring-up experiment performed immediately after the liquid was populated with bubbles (these bubbles are generated by the application for ~10 s of a sufficiently intense cavitation field sufficient to allow a cluster to form on the tip). In this case, a different acoustic signature and imaging data was obtained. Again a ~ 5 ms initiation period was observed. However, once the PLE starts to oscillate, the inherent bubble population

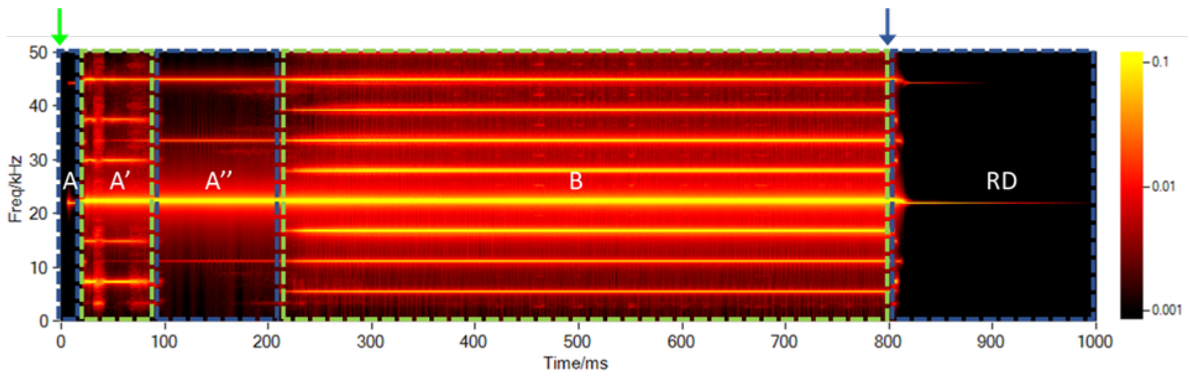

Figure 3. Plot shows the frequency components of the hydrophone signal, averaged over 10 repeat runs, and recorded as a function of time as the PLE was driven at a drive amplitude of 13 W_{rms} in soybean oil. The oil sample was cooled at 13 °C and pre-populated with gas bubbles through exposure to cavitation generated by the PLE. The panel is split into different time regions where the FFT analysis shows distinct behaviour (labelled A, A', A'', and B correlated to the discussion in the text). RD is where the PLE rings down. The PLE was driven for a time period of ~800 ms. Intiated at 0 ms (green arrow) and then switched off at ~ 800 ms (blue arrow). The scale bar represents voltage for the frequency components calculated from the hydrophone voltage time data.

(highlighted in Figure 2 panel (b)), results in the initiation of bubble related emissions after only ~ 30 ms. At this point a stable cluster was observed with a periodicity of *f*/3 (see Figure 2, panel (a) section A'). Again, the high-speed imaging indicates that this was as a result of a stable cluster with a matching periodicity (see Figure 2, panel (c)). This cluster is stable for ~70 ms until the set of subharmonics disappear (see Figure 2 panel (a), section A''). In this region the high-speed imaging indicates a bifurcation of the resulting streamer (see Figure 2 panel (d), white arrows showing the two streams detected). This unusual event has been described previously[22] and results from two bubble clusters formed at the tip of the HIU tip and oscillating out of phase. The position of the bifurcated streamer appears associated with surface functionality on the PLE tip (see SI data). Under these conditions this bifurcated streamer lasts ~ 50 ms before a sequence consisting of a cluster with *f*/4 periodicity (Figure 2 panel (a) section B), a mixed region (section C) and then finally a cluster with *f*/5 periodicity (section D) were detected. Clearly this should be put into the context of the experimental solution conditions and the characteristics of the PLE.

First, if the liquid oil is relatively bubble free, Figure 1 shows that the tip can ring-up to a relatively high displacement amplitude before any bubble events are generated. However, after nucleation and population of the liquid with bubbles has occurred (as in figure 2), the cluster initiates and immediately forms at a period of *f*/4 followed by a mixed region then finally an *f*/5 period. Second, if the oil is populated with a pre-existing bubble population, a variety of different stages at the beginning of the sequence were observed. If it is assumed that the displacement amplitude of the PLE ring-up is the same for both cases; this indicates that the *f*/3 and bifurcated streamer are only possible at lower tip amplitudes. The 'bubble free' experiments (see Figure 1 for example) do not offer these pre-existing nucleation points (bubbles) and hence these cluster periodicities will not be observed under those conditions with lower tip amplitudes. When bubble nucleation finally occurs, the tip amplitude is such that the higher order clusters

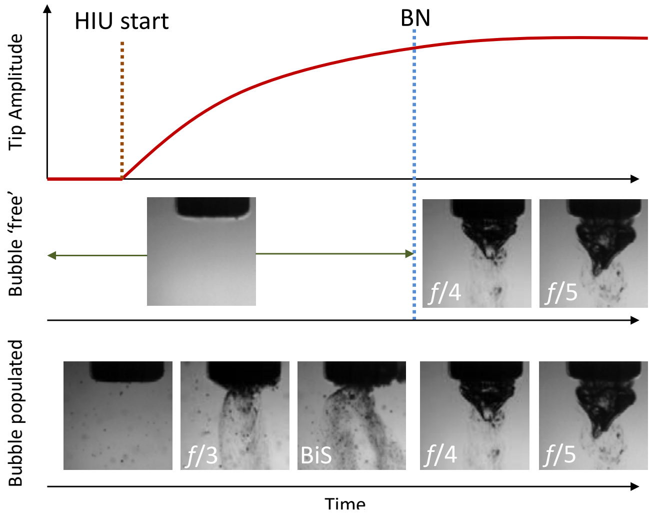

Figure 4. Schematic representation of the 'jump-in' mechanism. If a bubble free oil is employed, the tip amplitude rings up for a considerable period until a nucleation event (here labelled 'BN' or bubble nucleation) is detected. At this point an *f*/4 cluster is the first generated as the tip amplitude is sufficient to sustain this behaviour. In this case no lower order clusters are seen (including the BiS event). In a bubble populated oil, all the lower order clusters are sequentially accessed as the pre-existing bubble population negates the lag associated with the nucleation event.

are generated immediately. This 'jump in' mechanism is represented schematically in figure 4. The BiS event is easily identified within the hydrophone waveform by a clear reduction in the signal voltage (See SI data) compared to both the preceding *f*/3 and succeeding *f*/4 clusters. This event was found to be highly reproducible as long as an aged tip was employed. It was found that the BiS event could be generated in many oil systems (results not shown) and be produced using different apparatus (although with similar tip sizes and surface functionality).

It was also noted that the duration of BiS event varied considerably with the conditions of the experiment. To characterise this, a set of experiments where performed to investigate the lifetime of the BiS event as the oil temperature was varied. Figure 3 shows an example of frequency components detected in the hydrophone data during an 800 ms excitation experiment for one such experiment. Note the oil is populated and under the conditions employed rings up to form a final cluster with a periodicity of *f*/4. As seen previously, a set of subharmonic acoustic emissions were detected ~20 ms after the PLE was initiated, and corresponds to a cavitation cluster with a periodicity of *f*/3 (see Figure 3 section A') which remained stable for ~70 ms. Under the conditions employed, the bifurcated streamer (BiS) event was present for ~110 ms (see Figure 3 section A'') before an acoustic emission corresponding to a stable cluster with *f*/4 periodicity was observed (see Figure 3 section B). The PLE was switched off for the last 200 ms of the 1000 ms data capture window (see Figure 3 section C). During this

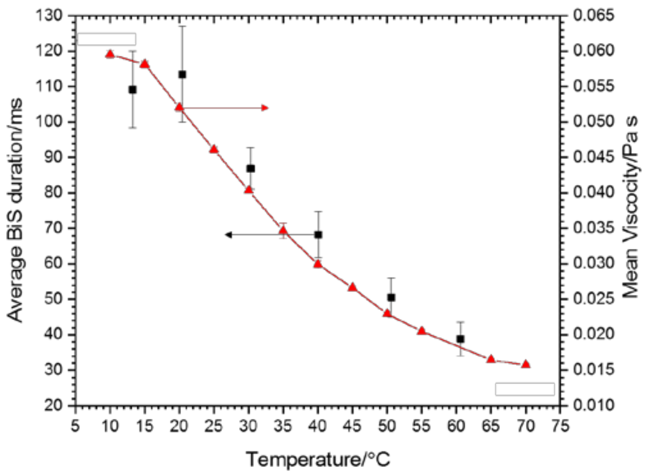

Figure 5. Plot displaying viscosity of SBO as a function of temperature (▲) between approximately 13-70 °C. The error bars represent the 95% confidence interval. Average bifurcated streamer region duration as a function of temperature (■) overlaid for comparison. The error bars were calculated for 80 repeat runs. The HIU tip was driven at 13 W_{rms} in all cases.

period the PLE 'rings-down' and the set of subharmonic frequencies disappear. Repeating this PLE ring-up experiment (up to 80 times per temperature – see SI data) and varying the temperature of the oil allows for a full set of data to be gathered with a degree of confidence.

Figure 5 shows a comparison of the BiS lifetime as a function of temperature. Plotted on the same graph is the viscosity of the SBO oil used in this experiment. Figure 5 shows that the lifetime of the BiS event drops as the temperature of the oil increases. In addition, features such as a plateau in the BiS lifetime at lower temperature in the range can be seen. This appears to correlate with the viscosity of the oil which shows very similar trends in its behaviour as a function of temperature. The lifetime of particular cavitation clusters, such as the unique BiS event reported here, could be critical to understanding the processes that occur within sonicated lipid samples at different supercooling temperatures[10,25,32,33]. Lastly, the nature of the populated media is of interest. Imaging experiments show that there are many bubbles present in the oil. These are generated through the population process (see figure 2, Image B) by exposing the oil to a cluster at high tip amplitude, for example. These bubbles are clearly visible and of many 10's μm in diameter. However, to access this population accurately is non trivial in this media and hence understand possible changes within it and their effect on the clusters within this system, more sophisticated experiments are required. This is beyond the current study and is part of ongoing work.

Conclusions

A sequence of stable cavitation clusters were investigated at an aged PLE tip in an oil/lipid system, each exhibiting a clear audible note that can be detected by ear. Complementary acoustic and high-speed imaging data shows that the pre-existing bubble population and the PLE tip displacement have a significant influence upon the observed cluster dynamics in the first 1000 ms of HIU treatment. A characteristic of the ring-up process in recently bubble populated media, is the presence of a bifurcated streamer (BiS). This unique double- or bi-cluster event is absent under bubble free conditions. Finally, the lifetime of the bifurcated streamer was reported to be highly temperature dependant, and was shown to decrease from ~114 ms to ~38 ms over a temperature range of 13-60 °C. This appears to correlate to the viscosity of the oil media employed.

Acknowledgements

This project was supported by Agriculture and Food Research Initiative (AFRI) Grant No. 2017-67017-26476 from the USDA National Institute of Food and Agriculture, Improving

Food Quality–A1361. This paper was approved by the Utah Agricultural Experiment Station as Paper Number 9279. We also thank the EPSRC (EP/D05849X/1) for funding related to the high-speed camera.

References

[1] A. Patist, D. Bates, Ultrasonic innovations in the food industry: From the laboratory to commercial production, Innov. Food Sci. Emerg. Technol. 9 (2008) 147–154. doi:10.1016/j.ifset.2007.07.004.

[2] P.R. Gogate, A.B. Pandit, Sonocrystallization and Its Application in Food and Bioprocessing, in: Ultrasound Technol. Food Bioprocess., Spinger, New York, United States, 2011: pp. 467–493. doi:10.1007/978-1-4419-7472-3_17.

[3] C.J. Price, Application of Ultrasound in Crystallization (Sonocrystallization), in: Eng. Crystallogr. From Mol. to Cryst. to Funct. Form, Springer, Dordrecht, Netherlands, 2017: pp. 301–313. doi:10.1007/978-94-024-1117-1_18.

[4] M.J.W. Povey, Applications of ultrasonics in food science - novel control of fat crystallization and structuring, Curr. Opin. Colloid Interface Sci. 28 (2017). doi:10.1016/j.cocis.2016.12.001.

[5] R. Chow, R. Blindt, A. Kamp, P. Grocutt, R. Chivers, Stimulation of ice crystallisation with ultrasonic cavitation - microscopic studies, Indian J. Phys. Proc. Indian Assoc. Cultiv. Sci. - Part A. 77A (2003) 315–318.

[6] H. Kiani, Z. Zhang, A. Delgado, D.-W. Sun, Ultrasound assisted nucleation of some liquid and solid model foods during freezing, Food Res. Int. 44 (2011) 2915–2921. doi:https://doi.org/10.1016/j.foodres.2011.06.051.

[7] S. Martini, R. Tejeda-Pichardo, Y. Ye, S.G. Padilla, F.K. Shen, T. Doyle, Bubble and Crystal Formation in Lipid Systems During High-Intensity Insonation, J. Am. Oil Chem. Soc. 89 (2012) 1921–1928. doi:10.1007/s11746-012-2085-z.

[8] W.L. Ng, C.H. Oh, A kinetic study on isothermal crystallization of palm oil by solid fat content measurements, J. Am. Oil Chem. Soc. 71 (1994) 1135–1139. doi:10.1007/BF02675908.

[9] S. Martini, Application of DSC, Pulsed NMR, and Other Analytical Techniques to Study the Crystallization Kinetics of Lipid Models, Oils, Fats, and Their Blends in the Field of Food Technology, in: Differ. Scanning Calorim. Appl. Fat Oil Technol., CRC Press, Florida, USA, 2015: pp. 163–195.

[10] A.H. Suzuki, J. Lee, S.G. Padilla, S. Martini, Altering functional properties of fats using power ultrasound., J. Food Sci. 75 (2010) E208-14. doi:10.1111/j.1750-3841.2010.01572.x.

[11] I. Foubert, P.A. Vanrolleghem, K. Dewettinck, A differential scanning calorimetry method to determine the isothermal crystallization kinetics of cocoa butter, Thermochim. Acta. 400 (2003) 131–142. doi:10.1016/S0040-6031(02)00484-7.

[12] Y. Ye, A. Wagh, S. Martini, Using high intensity ultrasound as a tool to change the functional properties of interesterified soybean oil, J. Agric. Food Chem. 59 (2011) 10712.

[13] S.D. Campbell, H. Douglas Goff, D. Rousseau, J.A. Rincón-Cardona, L.M. Agudelo-Laverde, M.L. Herrera, S. Martini, F. Chen, H. Zhang, X. Sun, X. Wang, X. Xu, Y. Ye, S. Martini, Application of High-Intensity Ultrasound to Palm Oil in a Continuous System, J. Am. Oil Chem. Soc. 81 (2015) 319–327. doi:10.1007/s11746-015-2620-9.

[14] M. Patrick, R. Blindt, J. Janssen, The effect of ultrasonic intensity on the crystal structure of palm oil, Ultrsonics Sonochemistry. 11 (2004) 251–255.

[15] K. Yasui, Acoustic Cavitation and Bubble Dynamics, Springer International Publishing, London, 2018.

[16] F.R. Young, Cavitation, Imperial College Press, London, 1999.

[17] E. Kirtil, M.H. Oztop, 1H Nuclear Magnetic Resonance Relaxometry and Magnetic Resonance Imaging and Applications in Food Science and Processing, Food Eng. Rev. 8 (2016) 1–22. doi:10.1007/s12393-015-9118-y.

[18] P.R. Birkin, D.G. Offin, P.F. Joseph, T.G. Leighton, Cavitation, shock waves and the invasive nature of sonoelectrochemistry, J. Phys. Chem. B. 109 (2005) 16997–17005. doi:10.1021/jp051619w.

[19] I. Hansson, V. Kedrinskii, K.A. Mørch, K.A. Morch, On the dynamics of cavity clusters, J. Phys. D. Appl. Phys. 15 (1982) 1725–1734. doi:10.1088/0022-3727/15/9/017.

[20] I. Hansson, K.A. Morch, The dynamics of cavity clusters in ultrasonic (vibratory) cavitation erosion, J. Appl. Phys. 51 (1980) 4651–4658.

[21] P.R. Birkin, T.M. Foley, T.T. Truscott, A. Merritt, S. Martini, Cavitation clusters in lipid systems-surface effects, local heating and streamer formation †, Phys. Chem. Chem. Phys. 19 (2017) 6785. doi:10.1039/c6cp08149e.

[22] P.R. Birkin, H.L. Martin, J.J. Youngs, T.T. Truscott, A.S. Merritt, E.J. Elison, S. Martini, Cavitation Clusters in Lipid Systems: The Generation of a Bifurcated Streamer and the Dual Collapse of a Bubble Cluster, J. Am. Oil Chem. Soc. 96 (2019) 1197–1204. doi:10.1002/aocs.12283.

[23] P.R. Birkin, T.M. Foley, T.T. Truscott, A. Merritt, S. Martini, Cavitation clusters in lipid systems – surface effects, local heating, outgassing and streamer formation, Phys. Chem. Chem. Phys. 19 (2017) 6785–6791.

[24] B. Esteban, J.R. Riba, G. Baquero, A. Rius, R. Puig, Temperature dependence of density and viscosity of vegetable oils, Biomass and Bioenergy. 42 (2012) 164–171. doi:10.1016/j.biombioe.2012.03.007.

[25] J. Lee, R.C. da Silva, V. Gibon, S. Martini, Sonocrystallization of Interesterified Soybean Oil: Effect of Saturation Level and Supercooling, J. Food Sci. 83 (2018) 902–910. doi:10.1111/1750-3841.14084.

[26] S. Martini, R. Tejeda-Pichardo, Y. Ye, S.G. Padilla, F.K. Shen, T. Doyle, Bubble and Crystal Formation in Lipid Systems During High-Intensity Insonation, J. Am. Oil Chem. Soc. 89 (n.d.) 1921–1928. doi:10.1007/s11746-012-2085-z.

[27] F. Chen, H. Zhang, X. Sun, X. Wang, X. Xu, Effects of Ultrasonic Parameters on the Crystallization Behavior of Palm Oil, J. Am. OIL Chem. Soc. 90 (2013) 941–949. doi:10.1007/s11746-013-2243-y.

[28] R. Jamshidi, D. Rossi, N. Saffari, A. Gavriilidis, L. Mazzei, Investigation of the Effect of Ultrasound Parameters on Continuous Sonocrystallization in a Millifluidic Device, Cryst. Growth Des. 16 (2016) 4607–4619. doi:10.1021/acs.cgd.6b00696.

[29] G.W.C. Kaye, T.H. Laby, Tables of Physical and Chemical Constants and some Mathematical Functions, 12th ed., Longmans, Green and Co, London, 1959.

[30] P.R. Birkin, D.G. Offin, C.J.B. Vian, T.G. Leighton, Multiple observations of cavitation cluster dynamics close to an ultrasonic horn tip., J. Acoust. Soc. Am. 130

(2011) 3379–88. doi:10.1121/1.3650536.

[31] D.G. Offin, Acoustoelectrochemical characterisation of cavitation and its use in the study of surface processes, University of Southampton, 2006.

[32] C. Himawan, V.M. Starov, A.G.F. Stapley, Thermodynamic and kinetic aspects of fat crystallization, Adv. Colloid Interface Sci. 122 (2006) 3–33. doi:10.1016/j.cis.2006.06.016.

[33] K. Sato, L. Bayés-García, T. Calvet, M.À. Cuevas-Diarte, S. Ueno, External factors affecting polymorphic crystallization of lipids, Eur. J. Lipid Sci. Technol. 115 (2013) 1224–1238. doi:10.1002/ejlt.201300049.